MELDOLA LECTURE. The Role of Aromatic Interactions in Molecular Recognition

Christopher A. Hunter
Department of Chemistry, University of Sheffield, S3 7HF, U.K.

1 Introduction

Interactions between aromatic molecules represent an important class of intermolecular force in chemistry, biology, and materials science. They control a range of molecular recognition and self-assembly phenomena such as:

(a) the packing of aromatic molecules in the crystalline state and hence the materials properties of these compounds;[1]
(b) the base-stacking interactions which determine the sequence-dependent structure and properties of DNA as well as recognition of DNA by drugs and regulatory proteins;[2]
(c) the three-dimensional structures of proteins;[3]
(d) molecular recognition of drugs by biological receptors or enzymes and of guests by synthetic hosts;[4,5]
(e) template-directed synthesis.[6]

I will use the term π–π *interaction* to describe non-covalent interactions between delocalized π-systems, including interactions between aromatic molecules.[7]

2 The Nature of π–π Interactions

Working with Jeremy Sanders in Cambridge, I began to study the properties of π–π interactions in covalently linked cofacial porphyrin dimers. These systems were originally designed as potential artificial enzymes, but strong π–π interactions between the two porphyrins forced the cavity to collapse and inhibited substrate binding. The geometry of the stacking interaction was determined from the ring current induced changes in the chemical shifts of the porphyrin ^{1}H NMR signals (Figure 1).[8] This geometry was unaltered when the porphyrins were metallated with zinc, but we were able to use these metallated dimers to determine the magnitude of the porphyrin–porphyrin π–π interaction. Bifunctional ligands such as DABCO can force the porphyrins apart by coordinating to both metal centres simultaneously. By comparing the thermodynamics of this binding interaction with model compounds, we determined the porphyrin–porphyrin interaction to be 48 ± 10 kJ mol^{-1} in chloroform (Figure 2).[9] This approach was subsequently extended to a number of other π–π interactions in related porphyrin dimers.

Armed with this experimental data, we set about trying to understand the nature of the π–π interaction. Molecular mechanics calculations using a number of force-fields consistently predicted that the low energy conformation for two stacked

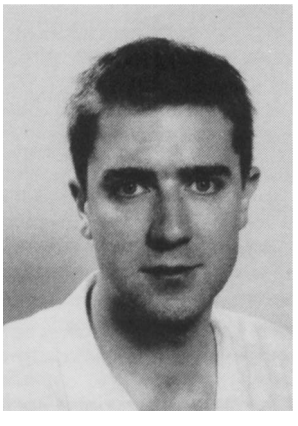

Chris Hunter was born in 1965. He obtained a B.A. in chemistry in 1986 from Churchill College, Cambridge, where he stayed to research with Dr. J. K. M. Sanders. He received a Ph.D. in 1989 and was then appointed to a lectureship in the University of Otago, Dunedin, New Zealand. In 1991, he moved to his current position in the Chemistry Department at the University of Sheffield. His research interests are in molecular recognition and supramolecular chemistry.

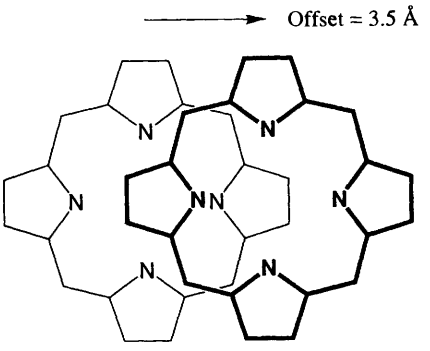

Figure 1 The geometry of the porphyrin–porphyrin stacking interaction observed in cofacially linked porphyrin dimers.

porphyrins is a perfectly aligned arrangement with maximum π-overlap rather than the experimental geometry in Figure 1. Clearly, there was something going on which was not accounted for by the molecular mechanics force-fields. If we think about any non-covalent interaction between two molecules, it involves the interplay of several different effects which can be divided into five categories:

(a) Van der Waals (VDW) interactions which are the sum of the dispersion and repulsion energies. These define the size and shape specificity of non-covalent interactions.
(b) Electrostatic interactions between the static molecular charge distributions. These are particularly important in conferring specificity on molecular recognition events.
(c) The induction energy which is the interaction between the static molecular charge distribution of one molecule and the proximity-induced change in the charge distribution of the other.
(d) Charge transfer which is a stabilization due to mixing of the ground state (AB) with an excited charge-separated state (A^+B^-).
(e) Desolvation. Two molecules which form a complex in solution must be desolvated before complexation can occur. The solvent may compete for recognition sites thereby destabilizing the complex. Alternatively in polar solvents, solvophobic effects can stabilize the complex.

There is clear experimental evidence that VDW interactions, electrostatic interactions, and desolvation play an important role in molecular recognition. However, there is not yet any experimental evidence that induction effects are as important. Charge transfer (CT) and electron donor–acceptor (EDA) effects are commonly invoked to explain interactions between aromatic molecules, but there is no evidence of CT in our porphyrin systems. Indeed, there is an increasing body of evidence which shows that CT and EDA effects are negligible compared with electrostatics.[10] In addition, *ab initio* calculations suggest that induction and CT energies are much smaller than electrostatic and VDW energies in non-covalent interactions between aromatic molecules. If we are to understand π–π interactions, we require the simplest possible model which is sufficiently complex to account for the experimental observations. We have therefore decided to ignore induction and charge-transfer effects in our analysis.

Let us therefore consider the three remaining effects listed above, VDW interactions, electrostatics, and desolvation. Aro-

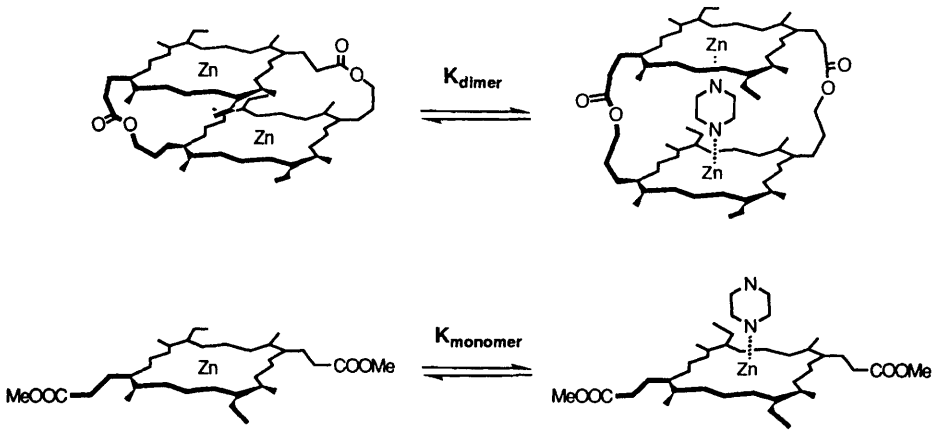

Figure 2 (a) A bifunctional ligand prises open a covalently-linked cofacial metalloporphyrin dimer (b) The control experiment used to determine the intrinsic binding energy associated with the zinc–ligand interaction By comparing $\Delta H_{monomer}$ with ΔH_{dimer} (and allowing for any cooperativity in binding both ends of the ligand), we can calculate the magnitude of the π–π interaction which is lost on opening the cavity in the porphyrin dimer, π–π interaction $= 2\Delta H_{monomer} - \Delta H_{dimer}$

matic molecules are planar so that VDW interactions are maximized when the molecules adopt a perfectly stacked arrangement The flat π-electron surfaces of the molecules are non-polar so that solvophobic effects also favour stacking [11] In addition, the porphyrin experiments described above were carried out in chloroform where solvophobic effects are small [12] Our experiments show that porphyrins prefer an offset or staggered arrangement This implies that the electrostatics of the interaction must provide a large driving force which pushes the π-systems away from optimal π-overlap These electrostatic interactions are clearly not present in molecular mechanics simulations, which generally use atomic monopole charge distributions, and suggests that a more detailed description of the charge distribution around π-systems is required to calculate the electrostatic interactions accurately [13]

We decided to use a charge distribution which explicitly represents the out-of-plane π-electron density which is characteristic of π-systems In our model, a positively charged σ-framework is sandwiched between two regions of negatively charged π-electron density (Figure 3) This model accounts well for the observed geometry and magnitude of the porphyrin–porphyrin stacking interaction (Figure 4) [7]

Encouraged by this success, we used this model to derive some general principles governing the properties of π–π interactions We examined interactions between simple three-centre charge distributions of the type shown in Figure 3 which we termed idealized π-atoms Figure 5 illustrates how the electrostatic interaction between two π-atoms varies as a function of orientation [7] The face-to-face stacked orientation (the origin in Figure 5) maximizes π-electron repulsion For edge-to-face and offset stacked orientations, attractive interactions between the positively charged σ-frameworks and the negatively charged π-

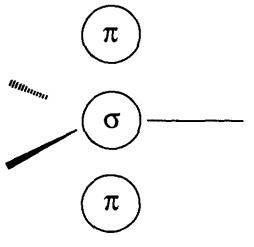

Figure 3 An sp^2-hybridized atom in a π-system

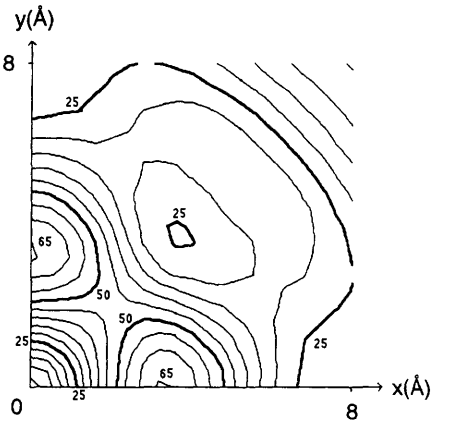

Figure 4 A contour plot showing the total interaction energy (in kJ mol^{-1}) for two stacked porphyrins as a function of translations in the xy plane (0 to 8 Å) The contour spacing is 5 kJ mol^{-1} Vertical separation of the porphyrins is 3 4 Å and there is no rotation of the porphyrins relative to one another Energy minima are labelled
(Reproduced with permission from the *Journal of the American Chemical Society*)

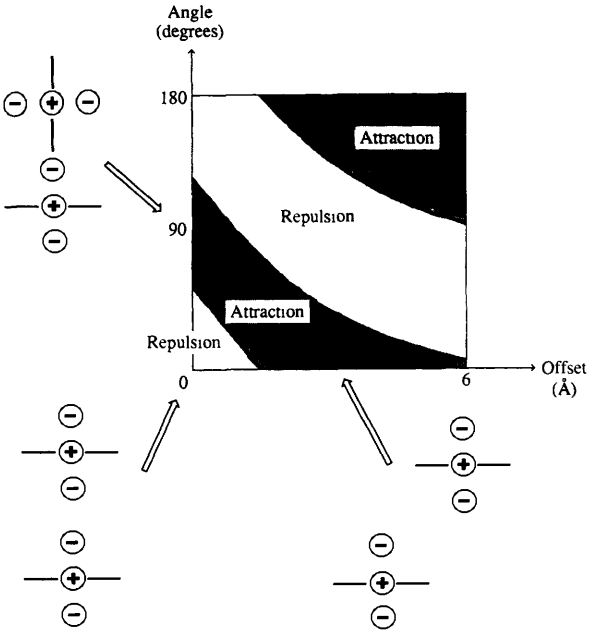

Figure 5 Electrostatic interaction between two idealized π-atoms as a function of orientation two attractive geometries and the repulsive face-to-face geometry are illustrated
(Reproduced with permission from the *Journal of the American Chemical Society*)

electrons dominate. Thus π-stacking is associated with large repulsive electrostatic interactions and is therefore much less favourable than one might expect on the basis of VDW interactions and solvophobic effects. The attractive edge-to-face and offset stacked interactions give rise to the characteristic herringbone packing of aromatic hydrocarbons in the crystalline state.[1]

The ideas summarized in Figure 5 hold for non-polarized π-systems, *i.e.* hydrocarbons which contain no heteroatoms. Polarization of the π-system by heteroatoms alters this picture and will be discussed later.

3 π–π Interactions in Proteins

Experimental evidence for the picture presented in Figure 5 comes from an analysis of the orientations of aromatic interactions in proteins. Singh and Thornton have compiled a database of the geometry of all side-chain–side-chain interactions in high resolution *X*-ray crystal structures of proteins.[14] We will concentrate on the interactions observed between the aromatic rings of phenylalanine (Phe) side-chains.[15] Figure 6(a) shows how the calculated electrostatic interaction between two benzene molecules varies as a function of orientation. This can be compared with the experimental distribution of Phe–Phe interaction geometries observed in the Singh–Thornton database [Figure 6(b)]. The experimental scatter maps out the region of conformational space which corresponds to an attractive electrostatic interaction. Orientations which would result in repulsive electrostatic interactions, such as face-to-face π-stacking, are not observed.

A strong clustering of experimental observations, which would indicate a deep well-defined energy minimum, is not observed. This is consistent with our calculations which indicate that the maximum electrostatic interaction is 6 kJ mol^{-1}. This is a rather weak interaction. However, aromatic side-chains often occur in clusters in proteins.[3] These clusters contain several π–π interactions and so make a significant contribution to the stability of that particular structural motif.

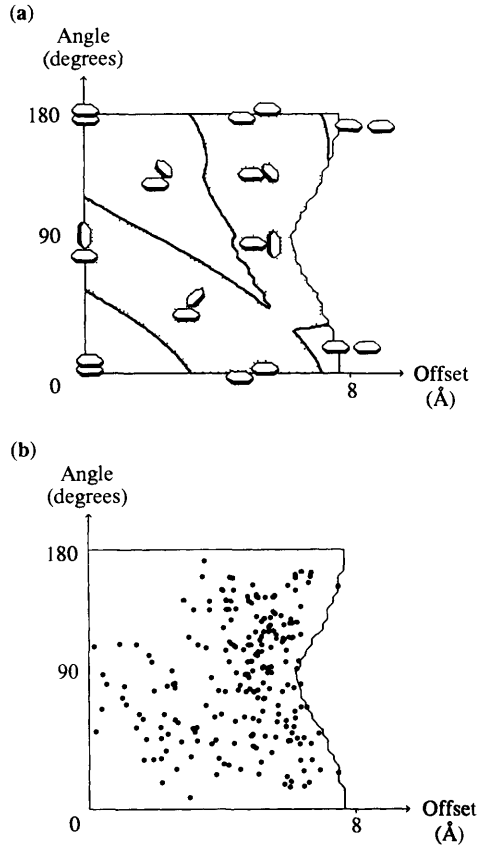

Figure 6 (a) Electrostatic interaction between two benzene rings as a function of orientation. The geometries of interaction are illustrated. The shaded area represents attractive interactions and the unshaded area represents repulsive interactions. (b) A scatter plot of the experimentally observed geometries of interaction between phenylalanine aromatic rings in proteins.
(Reproduced with permision from the *Journal of Molecular Biology*.)

4 π-Facial Hydrogen Bonds

If we consider π–π interactions in the wider context of electrostatic interactions between neutral molecules, which play an important role in molecular recognition, we have a heirarchy of electrostatic interactions with hydrogen bonds at the top and interactions between benzene rings at the bottom (this will hold in a vacuum, but solvent can influence this ordering). Intermediate between these two extremes, there are C-H···O hydrogen bonds (or C-H··· X hydrogen bonds, where X is an electronegative heteroatom) which have been extensively investigated[16] and π-facial hydrogen bonds which have surprisingly not received much attention (Figure 7).[17]

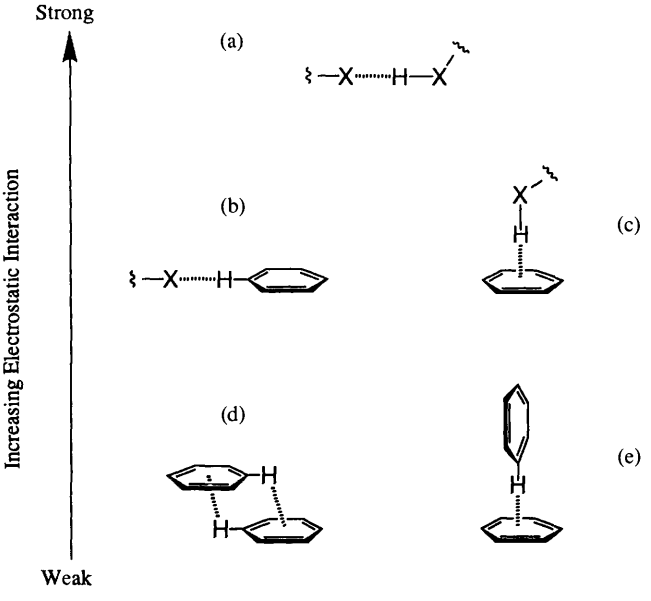

Figure 7 Heirarchy of electrostatic interaction between neutral molecules.
(Reproduced with permission from the *Journal of the Chemical Society, Chemical Communications*.)

Crystal structure databases such as that compiled by Singh and Thornton represent an excellent source of experimental data on the preferred geometries of non-covalent interactions. We therefore decided to search for π-facial hydrogen bonds in proteins using this database. The interaction which we chose was the arginine–phenylalanine side-chain interaction. Calculations using the electrostatic model discussed above predicted that the orientation with the edge of the guanidinium group hydrogen-bonded to the face of the phenylalanine π-system should be the most stable orientation, with a very well-defined energy minimum. However, the experimental data show that this geometry is extremely rare whereas almost every other orientation is highly populated. The reason for this discrepancy lies in the inhomogeneity of the protein environment. Our calculations were performed in a vacuum, but proteins contain many polar groups which can compete for the hydrogen-bonding sites on the arginine side-chain. A glance at Figure 7 shows that given the choice, a guanidinium proton will hydrogen bond to a proper hydrogen-bond acceptor [Figure 7(a)] rather than the face of a π-system [Figure 7(c)]. Proteins which contain an excess of hydrogen-bond acceptors, in particular amides, are therefore unlikely to show any π-facial hydrogen-bonding.

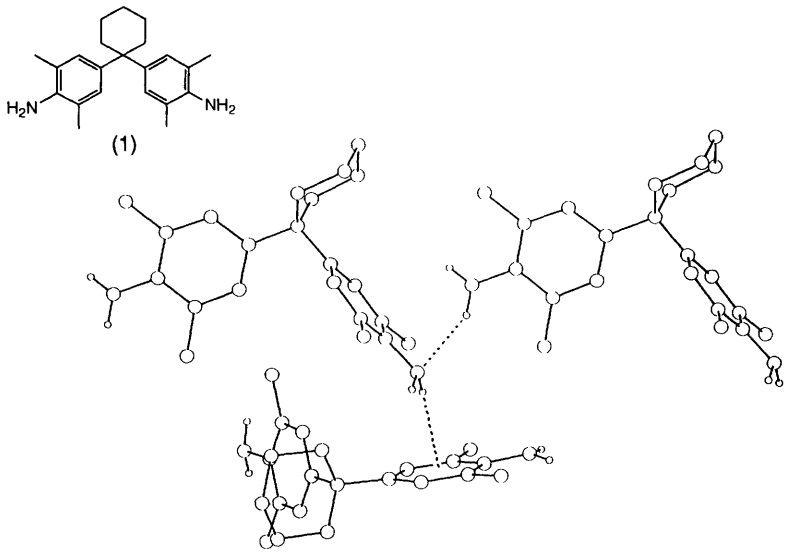

Figure 8 Intermolecular interactions observed in the crystal structure of (1). Hydrogen bonds are shown as dotted lines.
(Reproduced with permission from the *Journal of the Chemical Society, Chemical Communications*.)

We have studied a molecular assembly which does not contain any obvious hydrogen-bond acceptors, the crystal structure of an aniline derivative, (1). This system shows π-facial hydrogen-bonding involving an amine group directed into the centre of the face of an aromatic ring (Figure 8).[17]

5 Design of a Synthetic Receptor

In order to test these ideas further, I decided to design a synthetic host which would complex a guest using the edge-to-face π–π interactions which are predicted to be attractive.[18] I chose *p*-benzoquinone as the guest since I was interested in mimicking some of the properties of bacterial photosynthetic reaction centres where quinone cofactors play an essential role in the primary photoinduced charge-separation process.[19,20]

p-Benzoquinone has a range of possible recognition sites which could be exploited in host design [Figure 9(a)]. In order to select the optimum π–π interactions, we must consider the effects of the polarizing heteroatoms. The quinone carbonyl oxygens withdraw π-electron density from the ring. This will weaken an edge-to-face interaction with the face of the quinone π-system. In contrast, the polarization will enhance an interaction between the edge of the quinone and the face of another π-system. The host (2) which uses these edge-to-face interactions and maximizes the hydrogen-bonding interactions is illustrated in Figure 9(b).

Macrocycle (2) has been synthesized (see below), and it complexes *p*-benzoquinone with an association constant (K_a) of 10^3 M^{-1} in chloroform. Complexation-induced changes in the ^1H NMR chemical shifts of both the host and the guest indicate that the structure of the complex is as shown in Figure 9(b). These observations do not prove that there is an attractive π–π interaction in this system, but they are consistent with such an interaction. Moreover, (2) is selective for *p*-benzoquinone: substitution of methyl groups, chlorines, fluorines, or fused aromatic rings for the quinone hydrogens completely inhibits complexation ($K_a < 5$ M^{-1}). These changes would block the edge-to-face π–π interactions.

6 Template-directed Catenane Synthesis

The synthetic route to (2) produced the macrocycle, which will be referred to as the cyclic dimer, in 51% yield (Figure 10). However, there were two major side-products, a cyclic tetramer, (3), (10%) and a [2]-catenane, (4), (34%).[21] The catenated

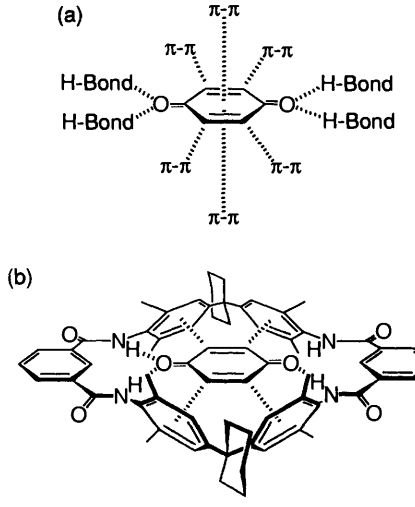

Figure 9 (a) Interaction sites available for molecular recognition of *p*-benzoquinone. (b) Complexation of *p*-benzoquinone by a synthetic macrocyclic host.
(Reproduced with permission from the *Journal of the Chemical Society, Chemical Communications*.)

product was completely unexpected, especially as the reaction was carried out under high dilution conditions (10^{-4} to 10^{-5} M). The three-dimensional structure of the catenane was determined using 2-D NMR and provides a clue as to why this self-templating process is so efficient.[21] There are a number of hydrogen bonds between the two interlocked macrocycles [Figure 11(a)] as well as several π–π interactions [Figure 11(b)]. The geometry of the π–π interactions is consistent with the model presented above. Each *i*-phthaloyl group bound inside the central cavity of the other macrocycle makes two offset stacked contacts and an edge-to-face contact with the aromatic side-walls of the cavity.

7 A Self-organizing Macrocycle

Neither (3) nor (4) complex *p*-benzoquinone. The cyclic tetramer adopts an open conformation [Figure 12(a)] and so does not have a cavity with dimensions suitable for *p*-benzoquinone recognition, and the catenane of course does not possess a cavity. When Duncan Purvis replaced *i*-phthaloyl dichloride by 2,6-pyridine dicarbonyl dichloride in the final cyclization step, he produced a similar set of macrocyclic products, but we were

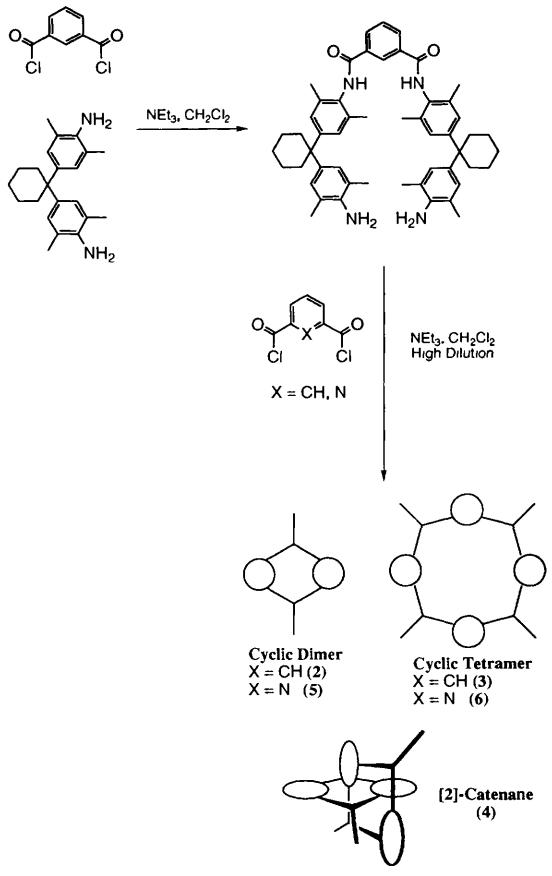

Figure 10 Synthetic route to amide macrocycles. The final macrocyclization step produces a cyclic dimer, a cyclic tetramer, and a [2]-catenane. (Reproduced with permission from the *Journal of the American Chemical Society*.)

surprised to find that both the cyclic dimer (5) and cyclic tetramer (6) formed complexes with *p*-benzoquinone.[22]

The NMR structure of the tetramer revealed the reason for this. Macrocycle (6) adopts a folded conformation in solution [Figure 12(b)] and so has two cavities complementary to *p*-benzoquinone. A titration showed that (6) binds two quinones with weak cooperativity [Figure 12(b)]. The interactions involved in recognition are again hydrogen bonds and edge-to-face π–π interactions. Macrocycle (6) has a covalent structure which differs only very subtly from that of (3), yet it adopts a completely different conformation and therefore has very different properties. The origin of this difference lies in the electrostatic interactions which control the conformational properties of the diamide subunits. 2,6-Pyridine diamides prefer a conformation with the amide NHs *cis*, because this minimizes lone pair repulsion and allows attractive electrostatic interactions with the pyridine nitrogen lone pair [Figure 12(b)]. In contrast, *i*-phthaloyl diamides prefer a conformation with the amide NHs *trans*, because this optimizes the electrostatic interactions between the two amide groups [Figure 12(a)].[22]

8 The Effect of Polarization by Heteroatoms on π–π Interactions

We have touched on the role of polarizing heteroatoms in modulating π–π interactions. The systems discussed in the first part of the paper were aromatic hydrocarbons which lacked heteroatoms. In these systems, face-to-face stacking is inhibited by π-electron repulsion. However, the introduction of polarizing substituents which perturb the molecular charge distribution changes this picture. Heteroatoms cause large partial atomic charges and lead to additional electrostatic interactions. We divide the electrostatic interactions in these systems into three categories:[2]

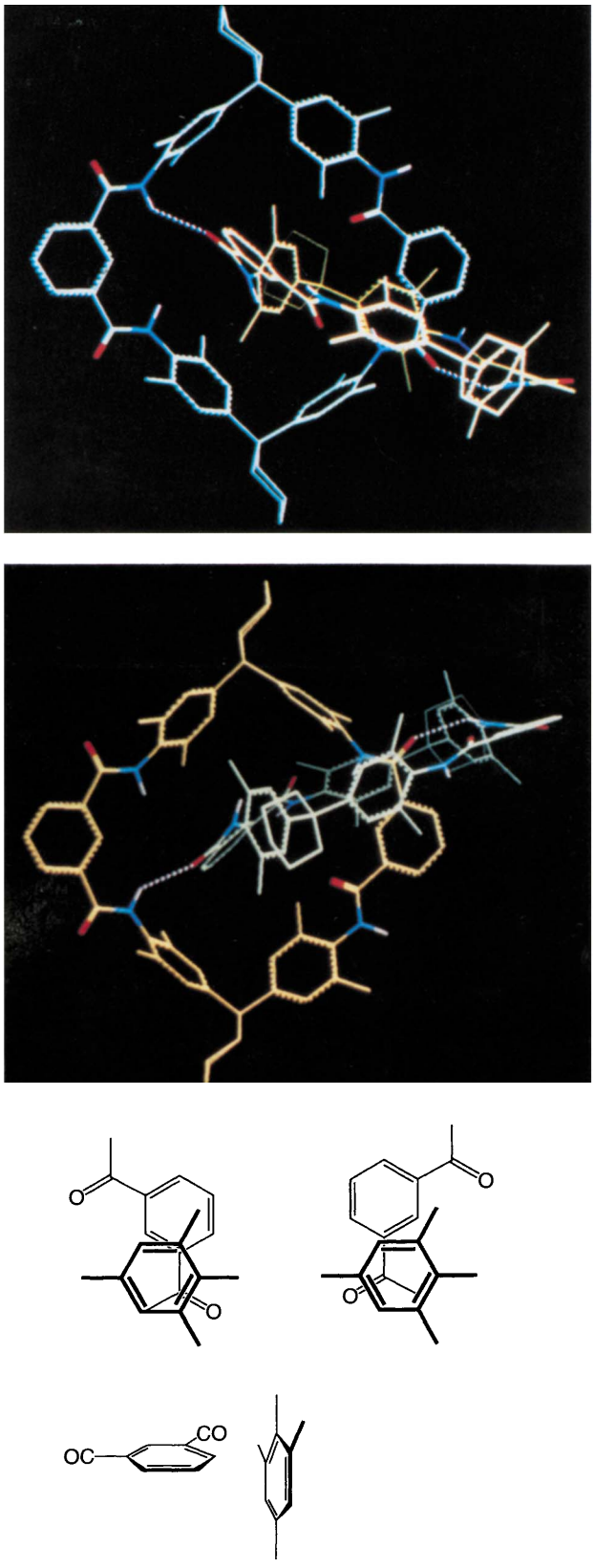

Figure 11 Interactions which help to interlock the two macrocycles of the [2]-catenane (4). (Top) The NMR-derived structure of the [2]-catenane which was energy minimized using the CHARMm force-field subject to NOE constraints. One macrocycle is coloured blue, the other yellow. Hydrogen bonds between the two macrocycles are shown as white dotted lines. (Bottom) Inter-macrocycle π–π interactions (two offset stacked and one edge-to-face interaction).
(Reproduced with permission from the *Journal of the American Chemical Society*.)

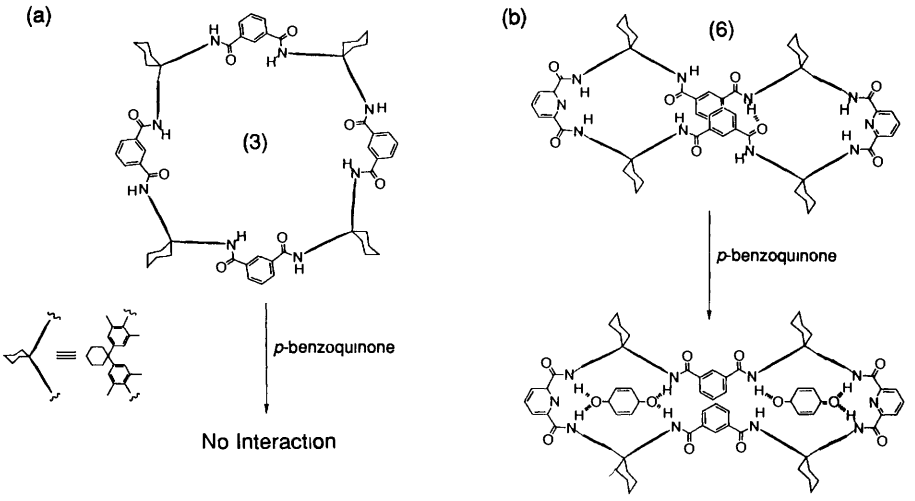

Figure 12 Preferred conformations and recognition properties of the tetrameric macrocycles (a) The tetra *t*-phthaloyl macrocycle (3) (b) The bis 2,6-pyridyl tetramer (6)
(Reproduced with permission from the *Angewandte Chemie International Edition in English*)

(a) $\pi\sigma$–$\pi\sigma$ interactions These are the interactions associated with the out-of-plane π-electron density if no polarization is present, *i e* the kind of interaction we have already discussed
(b) Atom–atom These are the interactions between the partial atomic charges
(c) Atom–$\pi\sigma$ This is the cross-term of the other two interactions, *i e* the interaction between the partial atomic charges on one molecule and the out-of-plane π-electron density on the other

For molecules which are highly polarized such as the DNA bases, $\pi\sigma$–$\pi\sigma$ interactions are not very important It is usually the atom–atom term which is the largest electrostatic interaction, but the atom–$\pi\sigma$ term can also be significant Moreover, the atom–$\pi\sigma$ term is very sensitive to changes in geometry and can play an important role in determining the orientation of π–π interactions between polarized π-systems

9 Sequence-dependent DNA Structure

The three-dimensional structures and properties of double helical DNA depend critically on the sequence of the aromatic bases Evidence comes from a wide variety of sources including, *X*-ray fibre diffraction studies of polymers,[23] *X*-ray crystal structures of oligomers,[24 25] gel running experiments,[26] and recognition of DNA by small organic molecules and proteins [25 27] An examination of the chemical structure of DNA shows that the only difference between different sequences lies in the aromatic bases [Figure 13(a)] The sugar-phosphate backbone is identical regardless of sequence It therefore follows that the cause of sequence-dependent variations in DNA structure is the π–π interactions between the aromatic bases which are stacked up the centre of the double helix

We have applied the π–π interaction model described above to elucidate the molecular basis for these structural variations [2] The conceptual basis for tackling this problem was established by Calladine and Drew [28] They showed how the conformation of a single base-pair step can be related to the overall three-dimensional structure of the double helix The conformation of a base-pair step can be defined in terms of six degrees of freedom (Figure 14) [29*] An analysis of DNA oligomer *X*-ray crystal structures shows that the parameters which are most important for defining sequence-dependent variations in structure are twist, slide, and roll [28] We have therefore analysed the π–π interactions for all ten possible base-pair steps as a function of these parameters The results correlate rather well with experiment and throw new light on many properties of nucleic acids, including the different conformational preferences of RNA and DNA, the formation of left-handed Z-DNA, and the role of TATA in originating replication

Inspection of the covalent structures of the bases (Figure 13) reveals that *all* sequence-dependent effects must be caused by
(a) steric interactions with the guanine amino group in the minor groove,

Figure 13 (a) The chemical structures of the DNA base-pairs C′ is the atom which connects the bases to the sugar (b) The molecular charge distribution of the base-pairs
(Reproduced with permission from the *Journal of Molecular Biology*)

* There are another six internal degrees of freedom for each base pair One of these parameters propeller twist (a rotation about the long axis of the base pair) plays an important role in defining sequence dependent changes in DNA structure but it will not be discussed here [2]

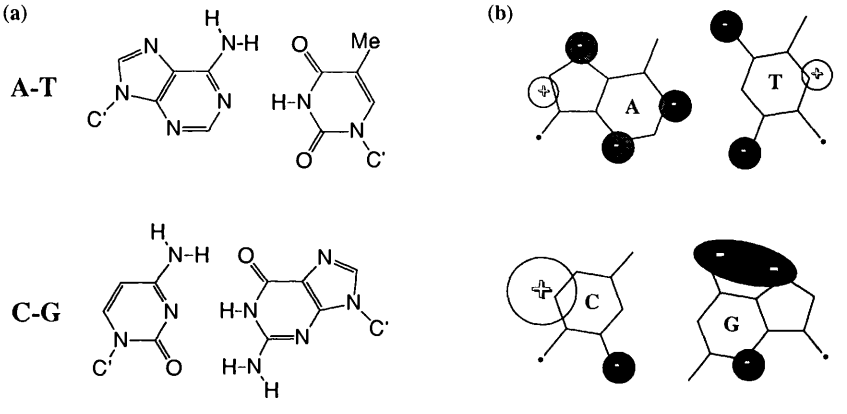

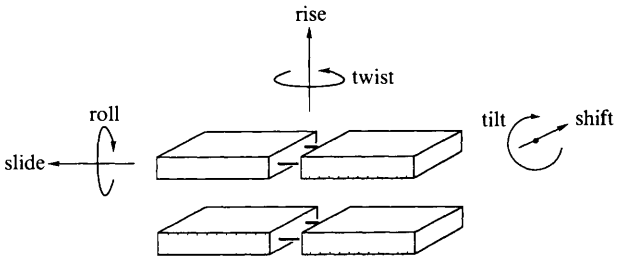

Figure 14 The conformation of a base-pair step in double-helical DNA can be defined by three rotations (twist, roll, and tilt) and three translations (rise, slide, and shift). The block edges which correspond to the minor groove are shaded.

(b) steric interactions associated with the configuration of the step, whether the sequence of bases is purine–purine, purine–pyrimidine, or pyrimidine–purine;
(c) steric interactions with the thymine methyl group in the major groove;
(d) electrostatic interactions associated with the different molecular charge distributions across the A–T and C–G base-pairs [Figure 13(b)].

The first two effects have been discussed in detail by Calladine and Drew.[28,30] Their observations are reproduced by our calculations, but in this paper we will concentrate on the last two effects. We will consider just two base-pair steps to illustrate the approach. A detailed analysis of the conformational properties of all ten base-pair steps can be found in reference 2.

Two base-pair steps which have been thoroughly characterized by experiment are AA/TT and CC/GG. These steps exemplify the two most common conformational families which were first observed by fibre diffraction methods, the A and B polymorphs. AA/TT has a very strong preference for the B-form (roll $\approx 0°$ and slide ≈ 0 Å).[23,26,31] CC/GG has a very strong preference for the A-form (roll $\approx 12°$ and slide ≈ -1.5 Å).[23,32] Why is this?

Contour plots of the magnitude of the π–π interaction between the base-pairs as a function of slide and roll are shown in Figures 15 and 17. The calculation for AA/TT shows a deep well-defined energy minimum at the origin (slide = 0 Å and roll = 0°), the region of conformational space which corresponds to the B-form that is observed experimentally (Figure 15). Comparison of the VDW interaction energy with the total π–π interaction energy shows that the conformational properties of this step are dominated by steric effects. Electrostatics are relatively unimportant because the AT molecular charge distribution has no large regions of high charge density.

The major steric interaction which locks AA/TT into the B-form is a clash between the thymine methyl group and the 5′-

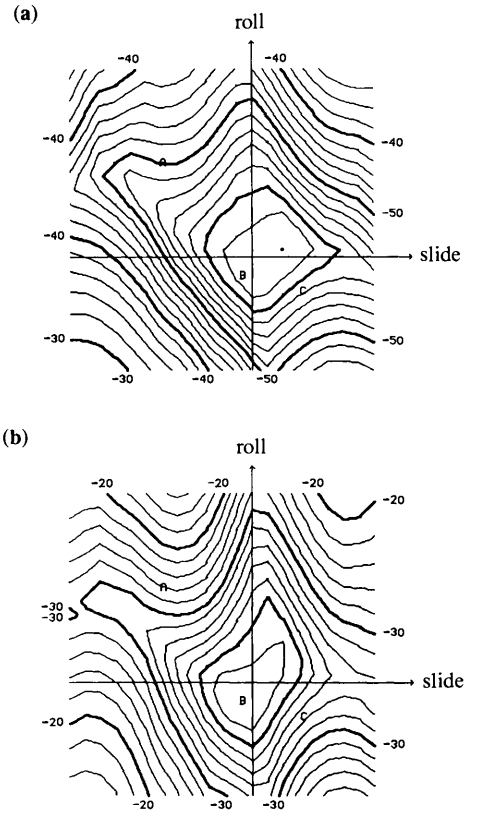

Figure 15 Contour plots showing the interaction energy for the AA/TT step (in kJ mol^{-1}) as a function of slide and roll. The contour spacing is 2kJ mol^{-1}. The slide axis runs from -3 Å to 2 Å and the roll axis runs from $-15°$ to 25°. Helical twist = 36°, propeller twist = 15° and all other parameters are set to zero. Energy minima and conformations corresponding to A, B, and C-DNA are labelled. (a) VDW interaction energy; (b) total π–π interaction energy (VDW + electrostatic).
(Reproduced with permission from the *Journal of Molecular Biology*.)

neighbouring base which occurs in positive roll A-type conformations (Figure 16). This interaction also provides an explanation for the different conformational properties of double-helical DNA and RNA. RNA has uracil in place of thymine and so lacks the major groove methyl groups. Thus double-helical RNA has only been observed in the A-form,[33,34] whereas the A-form of DNA is destabilized by the thymine methyl groups so that DNA is polymorphic.[23]

Electrostatic interactions play a more important role in the CC/GG step. C–G base-pairs have two regions of very high charge density, a positive charge over cytosine and a negative charge over guanine [Figure 13(b)]. The VDW interaction for CC/GG shows a broad flat energy minimum close to the origin, the B-form [Figure 17(a)]. Addition of the electrostatic interaction moves the energy minimum to large negative slide, close to the A-type conformation, in agreement with the experimental results for this sequence.

When the calculations were repeated omitting the out-of-

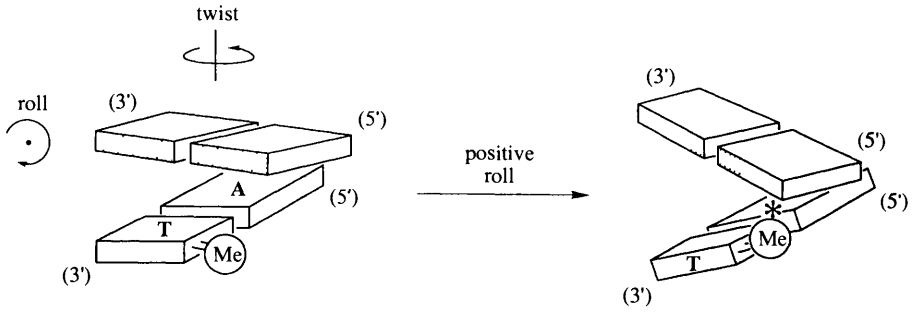

Figure 16 An AX/XT step viewed along the slide/roll axis (X is any base). The direction of positive slide is towards the reader. The block edges which correspond to the minor groove are shaded. The thymine methyl group prevents positive roll. Increasing roll leads to a steric clash (asterisk) between the thymine methyl and the other base on the same strand.
(Reproduced with permission from the *Journal of Molecular Biology*.)

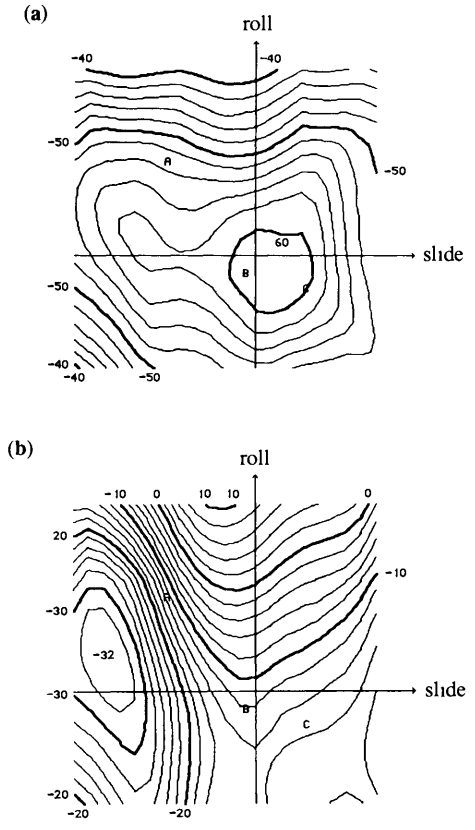

Figure 17 Contour plots showing the interaction energy for the CC/GG step (in kJ mol^{-1}) as a function of slide and roll The contour spacing is 2 kJ mol^{-1} The slide axis runs from − 3 Å to 2 Å and the roll axis runs from − 15° to 25° Helical twist = 36°, propeller twist = 15° and all other parameters are set to zero Energy minima and conformations corresponding to A, B and C-DNA are labelled (a) VDW interaction energy, (b) total π–π interaction energy (VDW + electrostatic)
(Reproduced with permission from the *Journal of Molecular Biology*)

plane π-electron density and using only partial atomic charges to calculate the electrostatic interaction, a very broad flat energy minimum with no clearly defined conformational preference was obtained Clearly, it is essential to allow for out-of-plane π-electron density to model accurately the properties of π–π interactions even for these very highly polarized π-systems The important interaction which causes the negative slide A-type conformation for CC/GG is the atom–$\pi\sigma$ interaction Figure 18 shows that the A-form is associated with a movement of the π-electron density of the bottom base-pair away from the guanine negative charge and towards the cytosine positive charge

Thus calculations using this model for π–π interactions reproduce the experimental conformational preferences of different DNA sequences and allow us to probe the molecular basis for these properties [2]

10 Conclusion

These studies show that in order to understand or model non-covalent interactions between aromatic molecules, it is essential to consider electrostatic interactions involving the out-of-plane π-electron density The pictures presented in this paper show how the properties of π–π interactions can be understood simply on the basis of the shapes and charge distributions of the individual molecules It is clear that π–π interactions have quite strong geometrical requirements and are directional to a much greater extent than was previously thought They therefore play a very important role in controlling specificity in molecular recognition

11 References

1 G R Desiraju and A Gavezzotti, *J Chem Soc Chem Commun*, 1989, 621
2 C A Hunter, *J Mol Biol*, 1993, **230**, 1025
3 S K Burley and G A Petsko, *Science*, 1985, **229**, 23
4 F Diederich, *Angew Chem Int Ed Engl*, 1988, **27**, 362
5 A V Muehldorf, D Van Engen, J C Warner, and A D Hamilton, *J Am Chem Soc*, 1988, **110**, 6561
6 P L Anelli, P R Ashton, R Ballardini, V Balzani, M Delgado, M T Gandolfi, T T Goodnow, A E Kaifer, D Philp, M Pietraszkiewicz, L Prodi, M V Reddington, A M Z Slawin, N Spencer, J F Stoddart, C Vicent, and D J Williams, *J Am Chem Soc*, 1992, **114**, 193
7 C A Hunter and J K M Sanders, *J Am Chem Soc*, 1990, **112**, 5525
8 P Leighton, J A Cowan, R J Abraham, and J K M Sanders, *J Org Chem*, 1988, **53** 733
9 C A Hunter, M N Meah, and J K M Sanders, *J Am Chem Soc*, 1990, **112**, 5773
10 F Cozzi, M Cinquini, R Annuziata, and J S Siegel, *J Am Chem Soc*, 1993, **115**, 5330
11 W L Jorgensen and D L Severance, *J Am Chem Soc*, 1990, **112**, 4768
12 D B Smithrud and F Diederich, *J Am Chem Soc*, 1990, **112**, 339
13 S L Price and A J Stone, *J Chem Phys*, 1987, **86**, 2859
14 J Singh and J M Thornton, *J Mol Biol*, 1990, **211**, 595
15 C A Hunter, J Singh, and J M Thornton, *J Mol Biol*, 1991, **218**, 837
16 R Taylor and O Kennard, *J Am Chem Soc*, 1982, **104**, 5063
17 L R Hanton, C A Hunter, and D H Purvis, *J Chem Soc Chem Commun*, 1992, 1134
18 C A Hunter, *J Chem Soc Chem Commun*, 1991, 749
19 H Michel, O Epp, and J Diesenhofer, *EMBO J*, 1986, **5**, 2445
20 J P Allen, G Feher, T O Yeates, H Komiya, and D C Rees, *Proc Natl Acad Sci USA*, 1988, **85**, 8487
21 C A Hunter, *J Am Chem Soc*, 1992, **114**, 5303
22 C A Hunter and D H Purvis, *Angew Chem Int Ed Engl*, 1992, **31**, 792
23 A G W Leslie, S Arnott, R Chandrasekaran, and R L Ratliff, *J Mol Biol*, 1980, **143**, 49
24 H R Drew, M J McCall, and C R Calladine, in 'DNA Topology and its Biological Effects', Cold Spring Harbour, 1990, p 1
25 O Kennard and W N Hunter, *Angew Chem Int Ed Engl*, 1991, **30**, 1254
26 C R Calladine, H R Drew, and M J McCall, *J Mol Biol*, 1988, **201**, 127
27 A A Travers and A Klug, in 'DNA Topology and its Biological Effects', Cold Spring Harbour, 1990, p 57

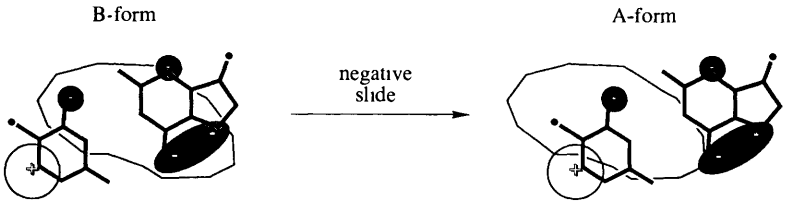

Figure 18 Atom–$\pi\sigma$ interaction in a CX/XG step (X is any base) The thin lines map out the area covered by the π-electron density of the X–X base-pair The molecular charge distribution of the C–G base-pair is shown • indicates the position of the C_1' atom where the bases are attached to the sugar
(Reproduced with permission from the *Journal of Molecular Biology*)

28 C R Calladine and H R Drew, *J Mol Biol*, 1984, **178**, 773
29 S Diekmann, *J Mol Biol*, 1989, **205**, 787
30 C R Calladine, *J Mol Biol*, 1982, **161**, 343
31 H C M Nelson, J T Finch, B F Luisi, and A Klug, *Nature*, 1987, **330**, 221
32 M McCall, T Brown, and O Kennard, *J Mol Biol*, 1985, **183**, 385
33 S Arnott, D W L Hukins, S D Dover, W Fuller, and A R Hodgson, *J Mol Biol*, 1973, **81**, 107
34 A C Dock-Bregon, B Chevrier, A Podjarny, D Moras, J S de Bear, G R Gough, and P T Gilham, *Nature*, 1988, **335**, 375